Available online at www.sciencedirect.com
ScienceDirect
International Journal of Mass Spectrometry 272 (2008) 63–77
International Journal of Mass Spectrometry
www.elsevier.com/locate/ijms

Sulfur isotope ratio measurements of individual sulfate particles by NanoSIMS

Baerbel Winterholler [b,*], Peter Hoppe [b], Stephen Foley [c], Meinrat O. Andreae [a]

[a] *MPI for Chemistry (Otto Hahn Institute), Department Biogeochemistry, P.O. Box 3060, D-55020 Mainz, Germany*
[b] *MPI for Chemistry, Department Particle Chemistry, P. O. Box 3060, D-55020 Mainz, Germany*
[c] *Johannes Gutenberg University, Department Geosciences, Joh.-Joachim-Becher-Weg 21, D-55099 Mainz, Germany*

Received 13 September 2007; received in revised form 26 December 2007; accepted 2 January 2008
Available online 17 January 2008

Abstract

The sulfur isotopic compositions of barite ($BaSO_4$), anhydrite ($CaSO_4$), gypsum ($CaSO_4{\cdot}2H_2O$), mascagnite ($(NH_4)_2SO_4$), thenardite (Na_2SO_4), boetite (K_2SO_4), epsomite ($MgSO_4{\cdot}7H_2O$), magnesium sulfate ($MgSO_4{\cdot}xH_2O$) and cysteine (an amino acid) were determined with a Cameca NanoSIMS 50 ion microprobe employing a Cs^+ primary ion beam and measuring negative secondary ions. This ion microprobe permits the analysis of sulfur isotope ratios in sulfates on 0.001–0.5 ng of sample material, enabling the analysis of individual S-bearing particles with diameters as small as 500 nm. The grain-to-grain reproducibility of measurements is typically 5‰ (1σ) for micron-sized grains, <5‰ for submicron-sized grains down to roughly 500 nm, and <2‰ for polished thin sections and ultra microtome sections which were studied for comparison. The role of chemical composition (matrix effect) and sample preparation technique on the instrumental mass fractionation (IMF) of the $^{34}S/^{32}S$ ratio in the NanoSIMS has been investigated for different sulfates and one amino acid. The IMF varies by ~15‰ between the standards studied here, underlining the importance of a good understanding of the matrix-specific IMF correction in order to get precise S isotope data for very small samples such as aerosol particles. A good correlation between IMF and ionic radius of the cations in sulfates was found, permitting inference of IMF corrections for sulfates for which no isotope standards are available.

Keywords: Sulfur isotopic composition; NanoSIMS; IMF; Sulfate

1. Introduction

Sulfur isotope analysis of atmospheric aerosol is a well established tool for identifying sources of sulfur in the atmosphere, estimating emission factors, and tracing the spread of sulfur from anthropogenic sources in terrestrial ecosystems [1]. Single particle techniques of isotope analysis can enhance the power of this tool by providing complementary chemical, mineralogical, morphological and isotopic information on individual aerosol particles [2].

In recent years, analysis of sulfur isotope ratios by SIMS (ion microprobe) has become a standard tool for the study of geological samples and meteorites. Analytical procedures for the analysis of sulfur isotope ratios with the Cameca IMS1270 [3,4], Cameca IMSxf [5–11], SHRIMP [12–16] and NanoSIMS [17] have been developed. Except for the NanoSIMS analysis of interplanetary dust particles these studies were made with a spatial resolution of down to 20 μm and typically consumed some 1–5 ng of sample material. However, the bulk of atmospheric aerosol particles is around 1 μm in diameter and contains approximately only 0.002 ng of sample material per particle. The new Cameca NanoSIMS 50 ion microprobe can perform sulfur isotope analysis of individual particles down to 500 nm in diameter with as little as 0.001 ng of sample material (0.02 pg S). This performance is critical for the analysis of individual aerosol particles. In an earlier study [2] it was shown that the typical reproducibility of the NanoSIMS 50 ion microprobe technique for S isotope measurements of individual, micrometer-sized grains is 5‰ (1σ), and around 2‰ (1σ) for S-bearing minerals in polished sections and ultra microtome sections. As shown

* Corresponding author at: Max Planck Institute for Chemistry, Department Particle Chemistry, P.O. Box 3060, D-55020 Mainz, Germany.
Tel.: +49 6131 305 358; fax: +49 6131 305 483/579.
E-mail address: winterho@mpch-mainz.mpg.de (B. Winterholler).

1387-3806/$ – see front matter © 2008 Elsevier B.V. All rights reserved.
doi:10.1016/j.ijms.2008.01.003

Table 1
Typical precisions for $^{34}S/^{32}S$ ratio measurements by conventional (gas-source) techniques, conventional SIMS, and NanoSIMS

Phase	Conventional techniques			SIMS		
	Precision (1σ)	Sample size	Reference	Precision (1σ)	Sample size (ng)	Reference
Sulfides	Combustion ±0.1‰	0.02–1 mg	[31–34]	IMS ser. ±0.25–1‰	1–5	[4–7,11,18,22]
	Laser ICP-MS ±0.2‰	0.1 mg	[35]	SHRIMP ±1‰	10	[12,13,16,36]
	Laser gas-source ±0.2‰	0.2 μg	[37]	NanoSIMS ±2–5‰	0.001–0.05	[2,17]
	TIMS ±0.1‰	0.1 mg	[38]			
Sulfates	Combustion ± 0.1‰	0.3–1 mg	[31–34]	SHRIMP ±2‰	10	[12,16]
				IMS ser. ±2‰		[11,19]
				NanoSIMS ±2–5‰	0.001–0.2	[2]

later in this study, precision levels are a strong function of grain size and sample preparation method, and uncertainties are high compared to conventional analysis techniques (Table 1). However, it should be noted that the conventional analysis of aerosol particles gives an averaged isotopic composition of bulk samples which may consist of many different types of aerosol particles and, therefore, masks the individual isotopic signatures. Only the new single particle technique presented here gives information pertaining to the variation in isotopic signature of the individual particles that make up the bulk samples [2]. It provides additional degrees of freedom in the interpretation of results by differentiating between primary sulfate particles and secondary sulfate particles deriving from gas to particle conversion, heterogeneous reactions on deliquescent particles or in-cloud processing based on particle chemistry and morphology and isotopic signature.

In order to apply the new NanoSIMS technique to the study of atmospheric aerosol, the matrix-specific instrumental mass fractionation (IMF) [12,18] of a large number of aerosol relevant minerals, especially sulfates, needs to be studied. Previous research has focused on the IMF of sulfide minerals [7,12,15–20]. Studies including the investigation of the matrix-dependent IMF of sulfates and glasses by Cs^+ sputtering are few and were performed using SHRIMP [12,16] and Cameca IMS 1270 [19] instruments under high mass resolution conditions or using an extreme energy filtering technique on a Cameca IMS6f [11]. Due to the limited sample material available in aerosol grains, a high mass resolution (HMR) approach is favorable for the analysis of aerosol samples. In the NanoSIMS, unlike Cameca IMSxf instruments, the useful ion yield is high even under high mass resolution conditions, while the energy filtering technique would result in a strong decrease of the useful ion yield.

The work presented here focuses on S isotopic measurements with the Cameca NanoSIMS 50 ion microprobe and explores the relationship between the matrix-specific IMF of the S isotopes in different sulfates, which is essential for the study of atmospheric aerosols. This is the first step towards establishing an easy-to-use method to correct the IMF of sulfur isotopes measured by NanoSIMS in atmospheric aerosols. In this paper we investigate the grain-to-grain reproducibility and accuracy of single particle sulfur isotope analysis for different sample preparation methods suitable for atmospheric aerosol particles and study the matrix dependence of the IMF on a set of 9 different matrices.

1.1. Instrumental mass fractionation in SIMS analysis

Instrumental mass fractionation occurs at several stages during SIMS analysis, including sputtering, ionization, extraction, transmission of the secondary ions through the mass spectrometer and secondary ion detection, and comprises mass-dependent as well as mass-independent effects. The effects related to the sputtering process, the ionization and extraction are matrix-dependent and might also depend on the sample preparation method and grain topography. Effects related to the transmission of secondary ions through the mass spectrometer depend on instrument tuning and are largely constant throughout an analytical session. Effects related to the use of electron multipliers for sulfur isotope analyses with the NanoSIMS depend on the tuning of the different electron multipliers (HV, preamplifier/discriminator settings, quantum efficiency of the first dynode). In the multi-collection measurement mode this results in different detection efficiencies for the different isotopes. High S count rates lead to electron multiplier aging over an analytical session, thereby continually decreasing the detection efficiency of the detector with which ^{32}S is measured.

Mass-dependent fractionation discriminates in favor of the lighter isotope ^{32}S and occurs during the sputtering process itself [18], during extraction in the reaction zone above the sample [21], and during transmission in the mass spectrometer [21]. Hervig [20] has shown that the IMF of S-isotopic ratios is a strong function of the initial kinetic energy of the secondary ions, specifically for secondary ions with low initial kinetic energy (<10 eV). This may explain the high sensitivity of the IMF in the HMR approach to small changes in the extraction field geometry [22] as well as to changes in the sample matrix [18] when low-energy ions are measured. Previous studies of S-isotopic ratios have shown that variations in the IMF of the S isotopes due to matrix effects are of the order of a few percent, which is comparable to the expected range of $^{34}S/^{32}S$ ratios in aerosol samples. Therefore, knowledge of the matrix-specific IMF for all relevant aerosol mineral phases is essential for obtaining accurate results.

Mass-independent effects discriminate against the most abundant isotope, ^{32}S, and are related to the use of electron multipliers [23]. The effect of electron multiplier dead time is well known and can be corrected [23]. The same applies for electron multiplier aging [21], which can also be properly corrected. Quasi-simultaneous arrival (QSA) [23,24], however, is hard to correct and its influence on the S isotope measurements

should be minimized by keeping the transmission of the mass spectrometer comparatively low or by using a Faraday cup as the ion detector for the most abundant isotope. The latter possibility does not work for the analysis of submicrometer- and micrometer-sized grains because the ^{32}S secondary ion signal is too low. The effect of QSA is clearly visible in the NanoSIMS because of the high ionization and collection efficiency of sulfur. The ratio of secondary ions ejected to the number of impacting primary ions may be as high as 20% in extreme cases. In such conditions, the probability of getting more than one secondary ion of an abundant isotope per primary impact is not negligible. Simultaneously emitted ions of the same isotope may arrive at nearly the same time on the conversion dynode of the electron multiplier and are registered as a single pulse. Therefore, the registered number of counts for the most abundant isotope is slightly lower than the actual number of incoming ions.

2. Materials and methods

2.1. NanoSIMS measurements

The S isotope measurements were performed with the Cameca NanoSIMS 50 ion microprobe at the Max Planck Institute for Chemistry in Mainz. This instrument is characterized by a lateral resolution superior to that of the Cameca IMSxf and 1270/80 instruments (<100 nm for Cs^+ primary ions), high transmission for secondary ions (typically several 10% for isotope measurements of the light-to-intermediate-mass elements) and multi-collection capabilities (up to 5 isotopes can be analyzed simultaneously) [25]. It was installed at the Max-Planck-Institute for Chemistry in 2001 and has been extensively applied to the study of extraterrestrial materials (e.g., [26–28]). The application of the NanoSIMS to problems in atmospheric chemistry started only recently [2].

The data in this study were obtained in multi-collection detector mode by sputtering the sample with a ~1 pA Cs^+ primary ion beam focused into a spot of ~100 nm diameter. The primary ion beam was rastered over $2 \times 2\ \mu m^2$ around the center of individual grains, irrespective of grain size. Each analysis comprised 600 s of pre-sputtering and integration of secondary ion signals over 1200 cycles of 1 s each. Samples were coated with gold (with the exception of certain experiments for sample preparation method #1, see below) and energy centering was used to compensate for charging. The NanoSIMS is equipped with an electron gun for charge compensation which, however, was not used, for the following reasons: Certain sulfates, e.g., ammonium sulfate, decompose rapidly under electron bombardment. Since ammonium sulfate contributes significantly (20–60%) to the total aerosol sulfate in most aerosol samples a measurement procedure involving the electron gun is problematic for most aerosol samples. However, charging is not a severe issue for the application of the method to atmospheric aerosol particles as most atmospheric sulfate particles are found in the accumulation mode (0.1–2.5 μm diameter) and show no significant charging. For larger grains, where charging may occur, our measurements show that sufficiently precise corrections on the $^{34}S/^{32}S$ ratio can be made.

Secondary ions of $^{16}O^-$, $^{32}S^-$, $^{33}S^-$, $^{34}S^-$, and $^{36}S^-$ were simultaneously detected in five electron multipliers at high mass resolution. Secondary ion count rates varied from 500 cps to 60,000 cps for ^{32}S depending on grain size, grain matrix and grain topography. The detector deadtime is 36 ns and the S^- count rates were corrected accordingly. Typically, deadtime corrections are smaller than 1‰ and never exceeded 2‰ for ^{32}S. Low-energy secondary ions were collected. In order to reduce the QSA effect on the S isotope ratio measurements, the transmission was set to ~15–20%, lower than would have been necessary to achieve a mass resolution sufficient to separate ^{33}S from the ^{32}SH interference. The transmission was set to 15–20%, by sputtering a 10 μm field on a polished section or a large grain until a stable count rate was achieved with all slits of the mass spectrometer wide open. Then the energy, entrance, and aperture slits were closed in the order mentioned to decrease the secondary ion count rate to 15–20% of the original value. Typically this was accomplished by setting the energy slit at a bandpass of 20 eV, in combination with a 20 μm × 140 μm entrance slit and a 150 μm × 150 μm aperture slit. Under these analytical conditions, the number of secondary ions per primary ion impact K is typically 0.002–0.003 for $CaSO_4$, $CaSO_4 \cdot 2H_2O$, $MgSO_4$, $MgSO_4 \cdot 7H_2O$, $(NH_4)_2SO_4$ and cysteine. Using the formula derived based on poisson statistics by Slodzian et al. [24], the IMF due to the QSA effect is typically 1‰ to 1.5‰ for these samples. Only three matrices show a higher contribution of QSA to the IMF, namely, $BaSO_4$ ($K = 0.006$, 3‰), K_2SO_4 ($K = 0.008$, 4‰), and Na_2SO_4 ($K_{corr} = 0.0136$, 6.8‰). Relative to $BaSO_4$, our standard for data normalization (see below), uncertainties in the IMF of $^{34}S/^{32}S$ due to QSA are thus estimated to be smaller than ±2‰; only for Na_2SO_4 it is somewhat higher.

Two commercially available isotope standards (IAEA-SO5, IAEA-SO6) with certified composition, and seven synthetic sulfates and one amino acid with known but uncertified S-isotopic composition (Table 2) were used to study the matrix dependence of the IMF and to explore different sample preparation methods. The synthetic sulfates are not guaranteed for homogeneity in isotopic composition by the producer, but from the production pathway it is justified to assume a homogeneous isotopic composition. The sulfur isotope ratios of these standards were measured in two laboratories by conventional gas-source mass spectrometry (see Section 2.3). Several standards were analyzed in both laboratories.

This study concentrates on the $^{34}S/^{32}S$ ratio as the precision of the $^{33}S/^{32}S$ and $^{36}S/^{32}S$ ratios in small particles is limited. Measurement of $^{16}O^-$ turned out to be useful to identify the sulfates in the ion images.

The influence of the sample preparation method on the reproducibility of the S-isotopic analysis was tested, because one of the challenges in the analysis of coarse grained (micron-sized) samples is that not all measurement parameters are under the control of the operator. The extraction field geometry and the degree of charging can vary considerably from grain to grain or even within the same grain. This affects the angular and energy distribution of secondary ions and thus their trajectories through the mass spectrometer, which can lead to variations in the IMF. Choosing an appropriate sample preparation method is the only

Table 2
Calculated chemical composition (assuming ideal formula) and $\delta^{34}S$ values of standard minerals

Atom (%)	$BaSO_4$	$(NH_4)_2SO_4$	$CaSO_4{\cdot}2H_2O$	$CaSO_4$	K_2SO_4	Na_2SO_4	$MgSO_4{\cdot}xH_2O$ 1–2 wt.% H_2O	$MgSO_4{\cdot}7H_2O$	Cysteine
S	16.7	6.7	8.3	16.7	14.3	14.3	16.3	4.8	26.7
O	66.7	26.7	50.00	66.7	57.1	57.1	65.9	40.7	26.6
N		13.3							11.7
C									30.0
H		53.3	33.3				1.4	51.9	5.0
Ba	16.7								
Ca			8.3	16.7					
K					28.6				
Mg							16.3	4.8	
Na						28.6			
$\delta^{34}S_{VCDT}$ [‰]	SO-5 + 0.5 SO-6 −34.1	+2.9	+9.9	+6.6	9.8	5.4	−0.8	3.1	21.7

way to minimize these variations. The effect of this is demonstrated by an analysis performed on two $CaSO_4$ grains in Fig. 1. Grain B (bottom) shows the common case, in which areas in the center of a larger flat grain (denoted by 2 in the SEM image) show lower secondary ion intensities due to increased charging compared to the grain rim (denoted by 1). Grain A in Fig. 1 (top) exhibits a complex topography. There are planes perpendicular to the incoming primary ion beam (denoted by 1 in the SEM image), which show high secondary ion intensities, even though they are closer to the center of the grain and may be expected to show more charging. Tilted planes (denoted by 2) show considerably lower secondary ion intensities. These different behaviors are also reflected in the shape of the peaks when so-called "Secondary ion beam centering" (SIBC) is done. With SIBC the voltages on 3 deflection plate pairs in front of the entrance slit of the mass spectrometer are optimized to get the maximum secondary ion intensity. When performing a horizontal SIBC (varying deflector Cy) on the analysis area marked by

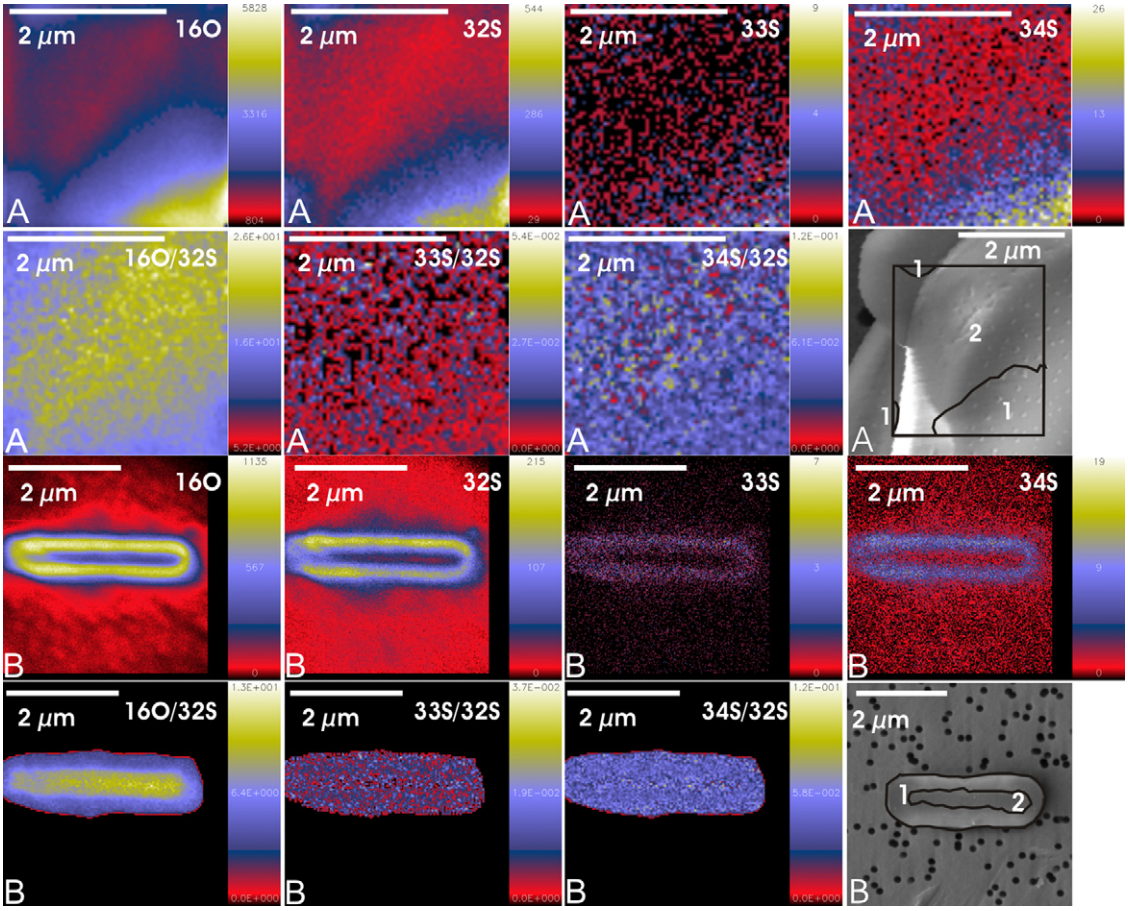

Fig. 1. Secondary electron microscopy and NanoSIMS ion images of two anhydrite grains. The field of view in the NanoSIMS image for grain A is 3 µm × 3 µm, that for grain B 4 µm × 4 µm. The position of the NanoSIMS analysis field on grain A has been marked (black rectangle) in the SEM image. "1" denotes areas with high secondary ion intensity, "2" denotes areas with low secondary ion intensity in both SEM images.

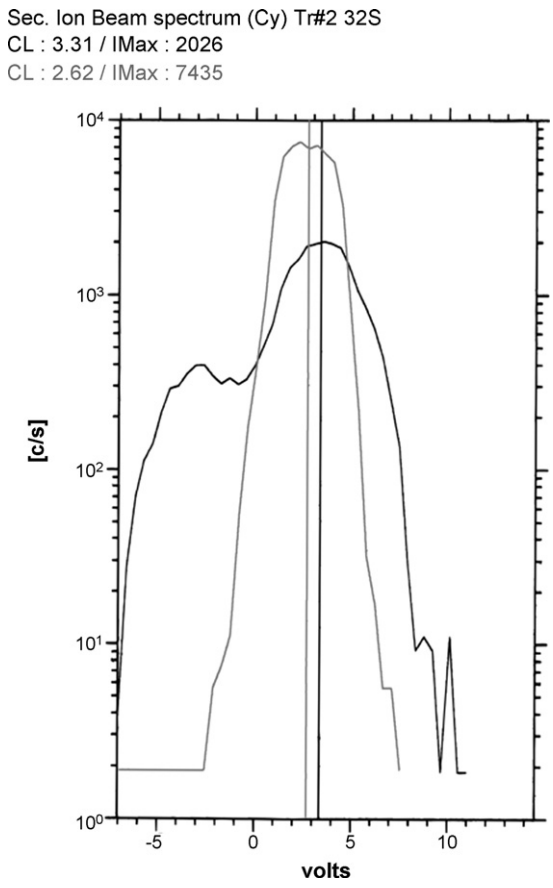

Fig. 2. ^{32}S intensity in different regions of grain A (see Fig. 1) as a function of the deflection plate voltage, Cy. Region inside the rectangle in the SEM image of grain A (Fig. 1): black. Region on flat surface in grain A: grey. See text for details.

the black rectangle in Fig. 1, a pronounced shoulder on the left side of the main peak is seen (Fig. 2, black curve), reflecting the complex topography of this analysis area. In contrast, the SIBC performed on a flat, horizontal analysis field, located only 1 μm to the right on the same grain, shows one narrow peak only (Fig. 2, grey curve). As can be seen from Fig. 2, not only the shape of the peaks different, but also the signal intensity and the position of the maximum. The latter underlines the importance of performing SIBC on each analyzed grain in addition to the energy and magnetic field centering which is commonly done.

This demonstrates that the charging and topography of grains present extreme challenges for precise S-isotopic measurements, in particular for the HMR technique, which has inherent limitations. For analyses on polished sections, Riciputi [22] found a point-to-point reproducibility of 0.5‰ for $^{34}S/^{32}S$ ratios as compared to 0.32‰ predicted by counting statistics for different spots on the same polished section. The reproducibility of $^{34}S/^{32}S$ ratios increased to 2.1‰ for the same standard mounted in several different polished sections. A better reproducibility may be achievable with the NanoSIMS if ^{32}S is measured with a Faraday cup. For grainy substrates, however, where grain charging and topography introduces additional uncertainties, the limit for the accuracy that can be reached for $^{34}S/^{32}S$ ratios is ≥2‰ (see below), even if the grains that are analyzed and the position of the analysis field on the grain are chosen with utmost care.

The topographic and charging effects may vary according to the sample preparation method. Therefore, we have explored the influence of the following four different sample preparation techniques on the IMF (Fig. 3):

1. Individual grains placed on gold-coated Nuclepore® filters to simulate the common experimental setup for the sampling of aerosol grains
2. Individual grains pressed into gold-coated Nuclepore® filters
3. Individual grains pressed into ultra-clean gold foils or onto stainless steel
4. Large (>15 μm) assemblies of grains pressed into ultra-clean gold foils

2.2. Sample preparation

2.2.1. Sample preparation method #1: individual grains placed on Nuclepore® filters

Aerosol samples for single particle analysis are typically collected on filters, such as Nuclepore® filters. As the filter background sulfur content is low, samples can be analyzed directly on this (Au-coated) filter. The integrated background contribution from the S^- signal on the empty filter is in most cases below 1% of the integrated S^- signal of individual aerosol particles [2]. Only if the particle thickness is <300 nm or the grain size <600 nm, the background contribution can be up to 10% of the total S^- signal. To facilitate the SIMS analysis and to prevent charging, filters are coated with gold from both sides before sample collection. In order to study the IMF of sulfur in different minerals under the same conditions as the real samples, standards were ground into fine powder and single grains of a given standard were placed on a Nuclepore® filter using a micro-manipulator. Grains were separated carefully in order to guarantee the analysis of individual grains. All filters, each containing different standards, were cut and one piece each was mounted on the same aluminum holder with Pelco conductive carbon tape. Two types of samples were prepared: (A) Coating of the grains with gold to ensure sufficient surface conductivity of the larger grains. (B) No coating of the grains with gold. Prior to ion microprobe analysis, the samples were characterized by scanning electron microscopy (LEO 1530 FESEM) and energy dispersive X-ray spectroscopy (Oxford Instruments EDX) to characterize the mineralogy (matrix), size and shape of individual grains. Grains with sizes between 1 μm and 15 μm were selected for analysis. The major advantages of type B samples are (i) that the identification and classification of grains by EDX is more accurate, as the gold interference on spectral lines of sulfur is less, and (ii) that carbonaceous aerosol grains can be identified as the carbon signal of the grains is strong compared to the carbon signal of the underlying polycarbonate filter which is shielded by the first gold coating. However, the major disadvantage of uncoated grains is that even comparatively small sulfate grains with diameters of <2 μm show an increased IMF in $^{34}S/^{32}S$ (Table 3) and a deteriorated grain-to-grain repro-

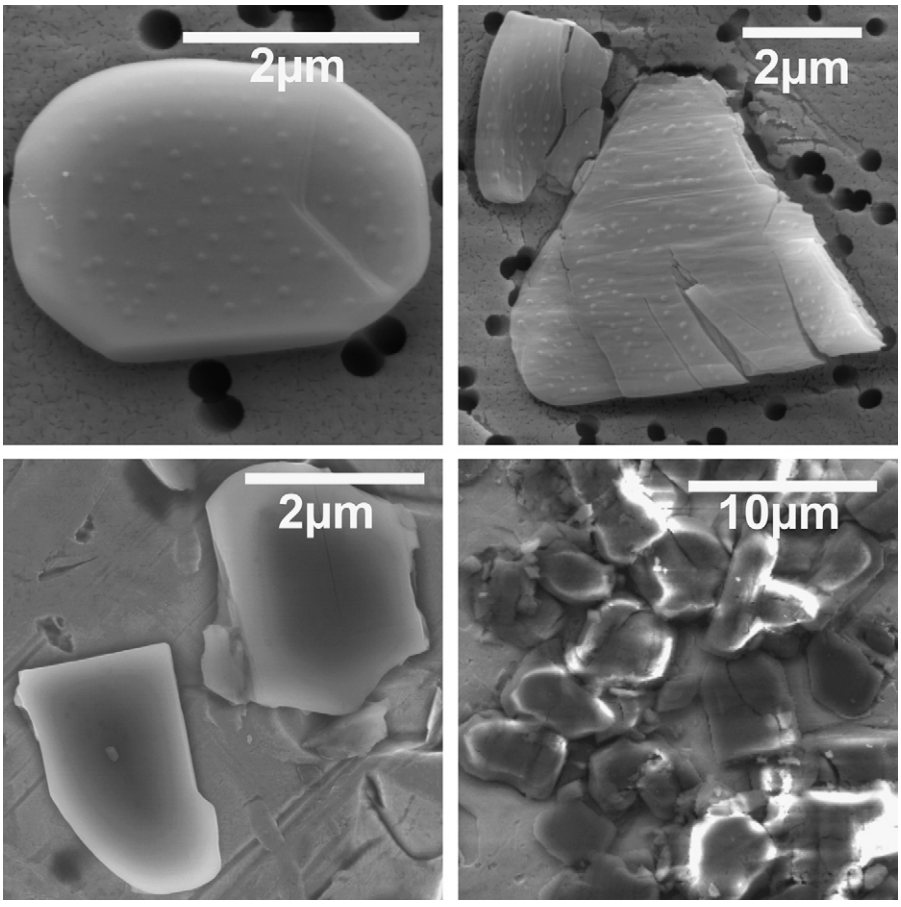

Fig. 3. Secondary electron microscope images of $CaSO_4$ standards illustrating the different sample preparation methods (#1: upper left, #2: upper right, # 3: lower left, and #4: lower right).

ducibility (Table 4). For larger grains the charging becomes so significant that successful analysis is no longer possible. Therefore, a gold coating on the particles is clearly preferred.

2.2.2. *Sample preparation method #2: individual grains pressed into Nuclepore® filters*

The powdered standards were placed on Nuclepore® filters according to method #1. Subsequently, the grains were pressed into the filter with a stainless steel stamp. In this way, the grains are partly embedded into the filter substrate and topographic effects are reduced. The further sample preparation is identical to that in method #1 (with Au coating of grains). The aim of this approach was to investigate whether comparatively flat samples will give a better reproducibility than the samples prepared with method #1.

2.2.3. *Sample preparation method #3: individual grains pressed into gold foil or onto the stainless steel*

The powdered standards were mounted on an ultra-clean gold foil at predefined locations. The imprint of a grid-pattern on the

Table 3
Matrix-specific IMF of $\delta^{34}S$ relative to $BaSO_4$ in eight sulfates and one amino acid for different sample preparation methods

Matrix	#1	σ	#2	σ	#3	σ	#4	σ	Not Au-coated		Predicted
									#1	σ	
$BaSO_4$ (IAEA SO5/O6)	0.8	0.6	−1.3	1.2	−1.0	0.9	−0.4	0.3	−6.0	2.1	−1.1
$CaSO_4$	−10.5	2.4	−8.3	1.9	−8.6	0.5	−21.1	1.0			−9.4
$CaSO_4{\cdot}2H_2O$	−9.4	1.5	−10.1	2.2	−9.9	0.5					−9.4
$(NH_4)_2SO_4$	−3.4	2.6					−6.9	2.4			−1.1
Na_2SO_4	−11.6	1.7									−11.1
K_2SO_4	−13.9	1.6									−3.3
$MgSO_4{\cdot}xH_2O$	−15.7	2.1									−15.6
$MgSO_4{\cdot}7H_2O$	−13.8	1.7									−15.6
Cysteine	−13.5	1.7									

Note: the IMF correction factor for $BaSO_4$ is the weighted average of both IAEA SO-5 and IAEA-SO-6 for all sample preparation methods used in any particular session. For that reason the calculated IMF of individual sample preparation methods can deviate slightly from 0. σ is the error of the weighted mean of the IMF determined in different measurement sessions. Predicted values are based on a relationship between measured $\delta^{34}S$ and ionic radius of cations in the sulfates.

Table 4
Grain-to-grain reproducibility σ_R (see Eq. (6)) of measured $\delta^{34}S$ values in different samples and for different sample preparation methods

Matrix	#1	#2	#3	#4	#1 not Au-coated	Thin and TEM section
$BaSO_4$	5.1	4.2	4.2	3.5	6.3	
$CaSO_4$	4.2	6.2	3.4	1.8		
$CaSO_4{\cdot}2H_2O$	3.4	2.3	4.4			
$(NH_4)_2SO_4$	7.1			4.2		
Na_2SO_4	7.1					
K_2SO_4	8.0					
$MgSO_4{\cdot}xH_2O$	5.6					
$MgSO_4{\cdot}7H_2O$	8.1					
Cysteine	6.7					
Mundrabilla Troilite (thin section)						<2
Interpl. dust particle (ultra microtome section)						<2

surface of the Au foil facilitates the relocation of the grains selected for NanoSIMS measurements. The grains were transferred with a micro-manipulator and pressed into the gold with a stainless steel stamp. In the same manner, standards were also mounted directly onto the clean stainless steel sample holder around aerosol filter samples. The whole mount was then coated with gold to ensure sufficient surface conductivity of the larger grains. Prior to ion microprobe analysis, the samples were characterized by SEM/EDX. Experiments involving the transfer of real aerosol samples onto gold foils have been performed to establish the feasibility of this approach. However, the transfer of individual aerosol particles is so time-consuming that it decreases the sample throughput significantly making this type of sample preparation unattractive.

2.2.4. Sample preparation method #4: large assemblies of grains pressed into gold foil

This sample preparation method is identical to method #3 except that large (>15 μm) grain assemblies were transferred to the Au foil. The transfer of individual grains with a micro-manipulator is very labor intensive. Handling of larger assemblies of grains that adhere to each other is much easier and faster. Therefore, if different standards with sufficiently large area for SIMS analyses need to be put together with the aerosol samples, this is the quickest technique. However, this approach can only be used if the IMF of S-isotopic ratios in larger assemblies of grains are comparable to that of individual grains, as the aerosol samples will usually consist of well separated particles.

2.3. Description and composition of standards

2.3.1. Barite ($BaSO_4$), thenardite (Na_2SO_4), and boetite (K_2SO_4)

Barium sulfate isotope standards IAEA SO-5 and IAEA SO-6 were obtained from the Isotope Hydrology Laboratory of the International Atomic Energy Agency, Vienna, Austria. The certified isotope composition of these standards is $\delta^{34}S_{VCDT} = +0.5‰$ (IAEA SO-5) and $\delta^{34}S_{VCDT} = -34.1‰$ (IAEA SO-6), respectively. The S-isotopic compositions of sodium sulfate anhydrous (VWR International, Leuven, Belgium) and potassium sulfate (Merck, Darmstadt, Germany) were measured using gas-source mass spectrometry which gave values of $\delta^{34}S_{VCDT} = 5.43 \pm 0.02‰$ and $9.79 \pm 0.01‰$, respectively (GPIM: Geologisch-Paläontologisches Institut und Museum der Westfälischen Wilhelms-Universität Münster, Münster, Germany).

2.3.2. Gypsum ($CaSO_4{\cdot}x2H_2O$) and anhydrite ($CaSO_4$)

Calcium sulfate dihydrate was purchased from Merck, Darmstadt, Germany. The $\delta^{34}S_{VCDT}$ value of this reagent was determined to be $9.8 \pm 0.2‰$ (DIGL: Department of Isotope Geochemistry, Centre for Environmental Research, Leipzig, Germany) and $9.91 \pm 0.04‰$ (GPIM), respectively. Calcium sulfate was procured from Alfa Aesar Johnson Matthey Company, Karlsruhe, Germany. Its sulfur isotopic composition was measured as $\delta^{34}S_{VCDT} = 6.42 \pm 0.15‰$ (DIGL) and $6.62 \pm 0.09‰$ (GPIM), respectively. The average volume loss of 17% from gypsum particles and a strong and long-lasting degassing of larger gypsum samples indicate that the crystal water degasses upon introduction into the UHV of the NanoSIMS chamber and the gypsum is converted to anhydrite. However, loss of crystal water does not influence the sulfur isotopic composition of the gypsum samples, as the IMF of anhydrite formed by degassing of gypsum grains and anhydrite purchased as such is always identical within the analytical error.

2.3.3. Magnesium sulfate ($MgSO_4{\cdot}xH_2O$) and epsomite ($MgSO_4{\cdot}7H_2O$)

Magnesium sulfate was purchased from Alfa Aesar Johnson Matthey, Karlsruhe, Germany. The $\delta^{34}S_{VCDT}$ value of this reference material was measured to be $-0.75 \pm 0.08‰$ (GPIM). Magnesium sulfate heptahydrate was procured from Merck, Darmstadt, Germany. The $\delta^{34}S_{VCDT}$ value of this reagent was determined to be $3.03 \pm 0.13‰$ (GPIM). Both magnesium sulfates undergo significant degassing and volume loss while losing their crystal water. It is not clear whether sulfur is lost in this process. If this were the case, variable loss of sulfur might lead to variable isotope fractionation and thus possibly to an apparent deterioration of the grain-to-grain reproducibility of S-isotope measurements. Also, if an isotope fractionation were to occur, the inferred matrix-specific IMF correction would be uncertain. However, no such deterioration of the grain-to-grain reproducibility has been observed for $MgSO_4{\cdot}xH_2O$ and only a slight deterioration is visible for $MgSO_4{\cdot}7H_2O$ indicating that

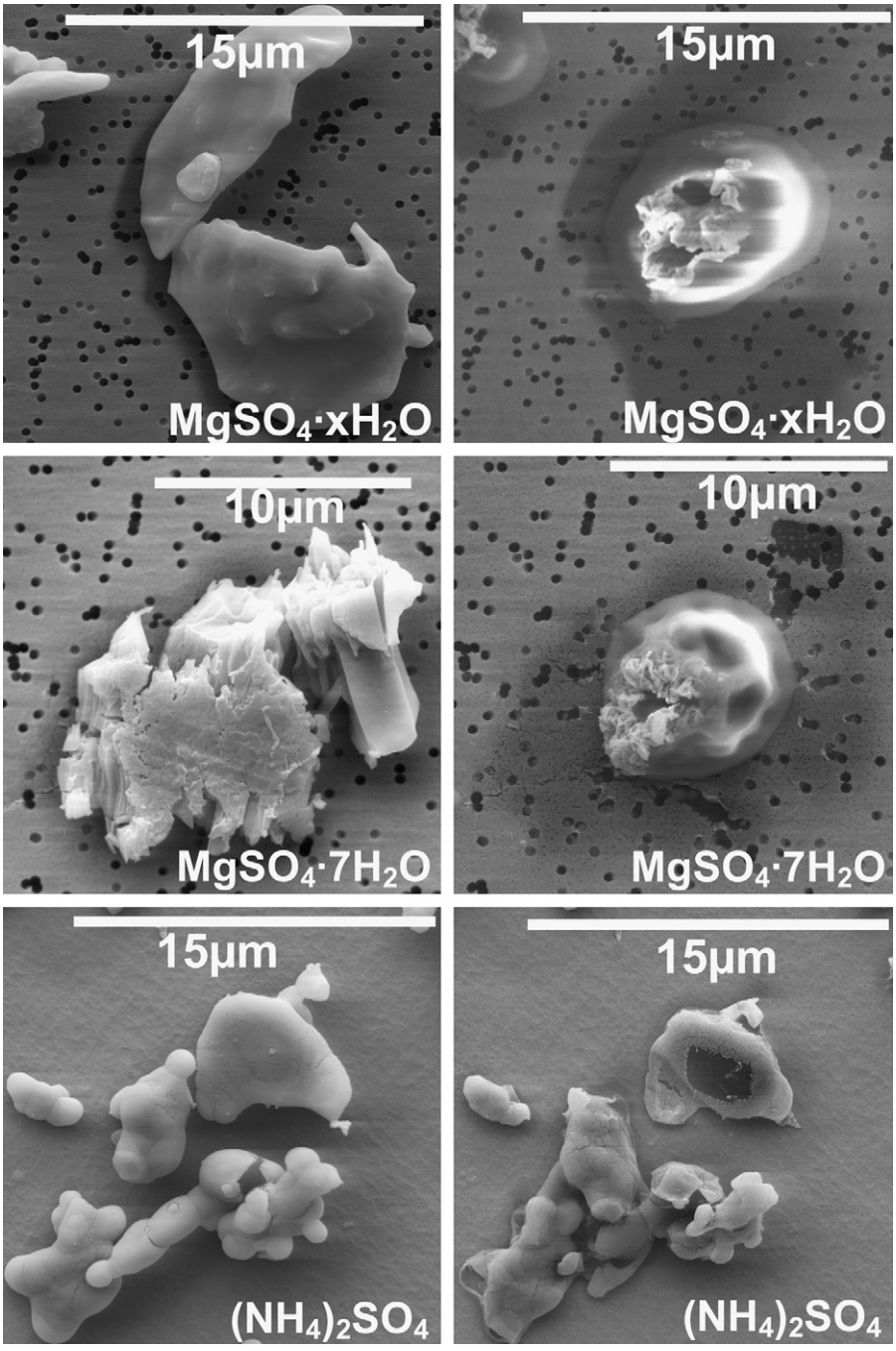

Fig. 4. Volume loss and recrystallisation of ammonium bisulfate particles illustrated by SEM images of the same particles taken before (left) and after (right) NanoSIMS analyses. Volume loss and recrystallisation of ammonium bisulfate is due to damage occurring under the electron beam and therefore depends on the electron dose the specific particle received. The NanoSIMS measurement field on the $(NH_4)_2SO_4$ grain (dark rectangle) is deformed from its original quadratic shape as the particle undergoes further decomposition while the image is being recorded.

loss of crystal water does not lead to any significant isotope fractionation, which is supported by our findings on gypsum (see Section 2.3.2).

2.3.4. Mascagnite ($(NH_4)_2SO_4$)

The $\delta^{34}S_{VCDT}$ value of ammonium bisulfate (Merck, Darmstadt, Germany) was measured as $+2.94 \pm 0.11‰$ (DICL). Ammonium bisulfate underwent significant decomposition and volume loss under the electron beam in the SEM, which depended on the time spent on imaging that particular particle. While standards from sample preparation method #4 can be analyzed without previous inspection in the SEM this is difficult for real aerosol samples. Standards that are treated like real samples (sample preparation method #1), show different degrees of decomposition and recrystallization for particles of which a close-up image was taken (i.e., for particles that received high electron doses (Fig. 4)). Even grains that were not analyzed in the NanoSIMS, but had been imaged in the SEM, show different degrees of volume loss 0 to >90%, depending on the electron dose they received during imaging. Grains

that were located by taking only short $55 \times 55\,\mu m^2$ overview images show no significant damage. The $\delta^{34}S$ values of individual grains that had been imaged in the SEM prior to the NanoSIMS analysis (sample preparation method #1) might thus be affected by variable isotope fractionation, which, depending on the amount of S loss, might affect the apparent grain-to-grain reproducibility. Furthermore, if an isotope fractionation had occurred, the inferred matrix-specific IMF correction for such grains would be uncertain. However, it is possible to investigate particles in the NanoSIMS without prior SEM analysis, as long as mineralogy (matrix), size and shape of individual grains are investigated after SIMS analysis. This requires that some of the grain is left for chemical analysis while the size can be derived from the overview image, used for the location of grains, albeit with a larger error (±0.3 μm for the particle diameter).

2.3.5. Cysteine

Standard reference material 143d cysteine (amino acid) was purchased from the National Institute of Standards and Technology (NIST, Gaithersburg, USA) in order to determine the IMF of S-isotopic ratios in organic material. The $\delta^{34}S_{VCDT}$ value of this material was measured as $+21.72 \pm 0.01‰$ (Geologisch-Paläontologisches Institut und Museum der Westfälischen Wilhelms-Universität Münster, Münster, Germany).

2.4. Instrumental mass fractionation correction

As mentioned earlier, IMF occurs at several stages during SIMS analysis, including sputtering, ionization, extraction, transmission of the secondary ions through the mass spectrometer and secondary ion detection. The IMF attributed to sputtering and ionization is matrix-specific [12,18]. The matrix-specific IMF of S-isotopic ratios was investigated for a set of 10 powdered reference materials and 9 different matrices, 8 sulfates and one amino acid.

All data presented here employ the δ notation relative to the appropriate international standard as follows [29,30]:

$$\delta^{34}S_{VCDT} = \left(\frac{(^{34}S/^{32}S)_{sample}}{(^{34}S/^{32}S)_{VCDT}} - 1 \right) \times 1000 \quad (1)$$

The absolute value of the instrumental mass fractionation factor α for the matrix x

$$\alpha(x) = \frac{(^{34}S/^{32}S)_{X,SIMS}}{(^{34}S/^{32}S)_{X,true}} \quad (2)$$

changes from session to session due to a variety of factors. Non-mass-dependent effects are introduced by changes in the sensitivity of the different electron multipliers (HV, preamplifier/discriminator settings, quantum efficiency of the first dynode). Additionally, instrumental tuning conditions (e.g., the blocking of the beam by slits) contribute to the IMF which is constant throughout a session but differs from session to session. These effects are not subject of our investigation and need to be eliminated in order to study the matrix-specific IMF and compare data obtained during different sessions. To compare relative differences between standards a relative matrix-specific IMF was established by defining the $\delta^{34}S_{bias}$ of barite to be zero and comparing all other standards to barite.

$$\delta^{34}S(x)_{bias} = \left(\frac{\alpha(x)}{\alpha(BaSO_4)} - 1 \right) \times 1000 \quad (3)$$

This is accomplished by multiplying the IMF of matrix x ($\alpha(x)$) with the inverse of the fractionation factor of $BaSO_4$ ($1/\alpha(BaSO_4)$). The weighted average of $1/\alpha$ for all $BaSO_4$ analyses in each measurement session is listed in Table 5. This weighted average includes all measurements in the respective session, irrespective of the number of sample preparation methods investigated and irrespective of changes in sample holders (e.g., during session 11/2005 two different standards were analyzed (IAEA-SO5 and IAEA-SO6), two different sample preparation methods were used (#1 and #4), and the standards were mounted on three different sample holders). Note that while the weighted average $\delta^{34}S(BaSO_4)_{bias}$ for the entire measurements session is 0 by definition this does not hold for the $\delta^{34}S_{bias}$ of individual grains on a specific mount (e.g., IAEA-SO5, mount 1) or individual grains of specific diameter, which can show a $\delta^{34}S_{bias}$ differing from 0.

It was discovered that for grains not pressed into the substrate (sample preparation method #1) the charging of the grains, and therefore the IMF of $^{34}S/^{32}S$, depends on the grain diameter. D_p is the equivalent diameter calculated as the diameter of a spherical particle occupying the same area as the analyzed particle, based on the number of pixels in the SEM image. The relationship IMF versus grain diameter was determined to be roughly the same for all standards with a change of $-1.6‰$ per μm increase in grain diameter D_p (Fig. 5). For the other sample preparation methods no significant dependence of the IMF on grain size was observed.

Therefore, for samples prepared according to method #1, the diameter of each grain as well as the average grain diameter $D_{p,m}$ of the $BaSO_4$ used for the correction of the IMF have to

Table 5
IMF correction factors for $^{34}S/^{32}S$ in $BaSO_4$

Session	$BaSO_{4\ true}/BaSO_{4\ SIMS}$	σ	$D_{P,m}$ (μm)
03/2006	1.0112	0.0026	1.9
01/2006	1.0092	0.0020	1.6
11/2005	1.0148	0.0012	3.2
10/2005	1.0106	0.0005	
09/2005	1.0122	0.0006	
08/2005	1.0317	0.0008	3.6
07/2005	1.0370	0.0017	
06/2005	0.9955	0.0019	
05/2005	0.9929	0.0010	
03/2005	0.9827	0.0020	
02/2005	1.0089	0.0007	

σ is the standard deviation of the correction factor in the respective analytical session. Also given is the average particle diameter $D_{p,m}$ for samples prepared by method #1. This is the only sample preparation method for which a noticeable grain size dependence of the IMF is evident.

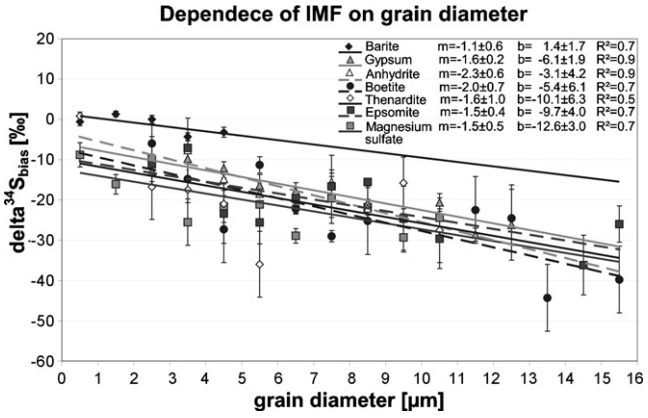

Fig. 5. Grain size dependence of the IMF of δ^{34}S in different sulfate standards prepared according to sample preparation method #1. The slopes observed for all standards agree within the errors. The weighted mean of all slopes is -1.6 ± 0.2‰/µm.

be incorporated into the formula:

$$\delta^{34}S(x)_{bias} = \left(\frac{\alpha(x)}{\alpha(BaSO_4)} \frac{1}{(a(D_{p,m} - D_p)/1000) + 1} - 1 \right) \times 1000 \quad (4)$$

Here, $\alpha(BaSO_4)$ is the weighted average over all grain sizes and $a = -1.6\ \mu m^{-1}$ for sample preparation method #1 and $a = 0$ for the other sample preparation methods.

The isotopic composition of sample X relative to the VCDT standard ($\delta^{34}S_{VCDT}$) is calculated taking into account the appropriate matrix-dependent mass fractionation ($\delta^{34}S(x)_{bias}$) for each specific grain using Eq. (4):

$$\delta^{34}S(x)_{VCDT} = \left(\frac{(^{34}S/^{32}S)_X}{(^{34}S/^{32}S)_{VCDT}} \frac{1}{\alpha(BaSO_4)} \frac{1}{(\delta^{34}S(x)_{bias}/1000)+1} - 1 \right) \times 1000 \quad (5)$$

The total error of the $\delta^{34}S_{VCDT}$ values (σ_T) is larger than the error estimated from counting statistics (σ_P) alone. This is evident when the standard deviation of the δ^{34}S values of all measurements in a given session for each type of sample is compared with the average counting statistical error. After subtracting the average counting statistical error ($\sigma_{P,m}$) from the standard deviation (σ), a residual error remains (σ_R). The residual error is a measure of the grain-to-grain reproducibility and can be calculated from

$$\sigma_R = \sqrt{\sigma^2 - \sigma_{P,m}^2} \quad (6)$$

for each standard. The total error (σ_T) of an individual measurement is then calculated based on the counting statistical error of that measurement itself and the residual error:

$$\sigma_T = \sqrt{\sigma_P^2 + \sigma_R^2}. \quad (7)$$

3. Results and discussion

The results of more than 500 NanoSIMS sulfur isotope measurements are summarized in Table 6. Additional information is available from the corresponding author on request. In Table 3 we list the average (over all measurement sessions) IMF of δ^{34}S relative to $BaSO_4$ for each standard and sample preparation method together with predictions from the observed relationship between IMF and ionic radius of cations in the sulfates (see Section 3.2). The $\delta^{34}S_{bias}$ values of the individual measurements are presented in Fig. 6. In Table 5 we give the IMF correction factors derived from the measurements on $BaSO_4$ for each of the 11 measurement sessions between February 2005 and March 2006 (calculated as weighted average) together with $D_{P,m}$ for samples prepared according to method #1. The IMF correction factors can be <1 or >1 because of different detection efficiencies for the different S isotopes in the multi-collection mode. These numbers are thus hard to compare with IMF factors of $BaSO_4$ in absolute terms measured in single collection mode. Therefore, values are normalized to $BaSO_4$ as mentioned above. The influence of the sample preparation methods on the IMF and grain-to-grain reproducibility σ_R was studied on barite, anhydrite, gypsum, and ammonium sulfate.

3.1. Influence of the sample preparation method

For $BaSO_4$ no significant difference in the IMF of $^{34}S/^{32}S$ was observed for the different sample preparation methods (Tables 3 and 6, Fig. 6). Only measurements on uncoated grains led to a distinctly more negative (by −6‰) IMF and a deteriorated grain-to-grain reproducibility compared to gold-coated samples, indicating that even for comparatively small grains with diameter of <2 µm conductive coating is important.

For anhydrite and gypsum, the average IMF of δ^{34}S relative to $BaSO_4$ is -9.3 ± 1.0‰ in samples prepared according to methods #1 to #3. No significant differences are observed between these sample preparation methods (Table 3, Figs. 6 and 7). For method #4, the IMF of anhydrite increases to −21‰ due to increased charging (Tables 3 and 6, Figs. 6 and 7). For gypsum, charging of samples prepared according to method #4 is so strong that energy centering is not sufficient for charge compensation and the secondary ion yields are too low for successful analysis. In each measurement session the IMF of gypsum was identical to that of anhydrite within the analytical errors.

For $(NH_4)_2SO_4$ a small difference in the IMF between the two investigated preparation methods (#1, #4) was observed, with slightly more negative values for sample preparation method #4. The grain-to-grain reproducibility of the measurements on samples from method #1 is very poor (∼16‰) for grains which were exposed to high electron doses in the SEM. Fractionation during the decomposition of the sample under the electron beam in the SEM might be responsible for this behavior. A slight dependence of δ^{34}S on the volume loss is evident from Fig. 8 for these particles. However, no such dependence and a grain-to-grain reproducibility of ∼7‰ are observed for par-

Table 6
Results of sulfur isotope analyses of different standards

Session	Sample prep. method	$^{34}S/^{32}S$	σ	$\delta^{34}S_{VCDT}$ (‰)	σ	σ_T indiv. meas.	#
$BaSO_4$ SO-6 $\delta^{34}S_{VCDT}$ −34.1‰							
03/2006	#1	0.04225	0.00005	−33.1	1.1	5.7	26
01/2006	#1	0.04227	0.00008	−33.8	1.5	5.6	15
11/2005	#4	0.04221	0.00014	−36.3	3.2	4.4	3
11/2005	#1	0.04192	0.00008	−33.7	1.7	6.6	16
10/2005	#4	0.04221	0.00002	−34.3	0.5	2.9	32
09/2005	#4	0.04216	0.00003	−34.8	1.0	4.7	24
08/2005	#1	0.04166	0.00003	−26.8	0.7	6.1	9
08/2005	#4	0.04114	0.00008	−38.9	1.8	3.0	4
02/2005	#4	0.04232	0.00003	−33.7	0.8	1.6	5
$BaSO_4$ SO-5 $\delta^{34}S_{VCDT}$ +0.5‰							
11/2005	#1	0.04394	0.00006	+4.6	1.4	2.5	3
11/2005	#1	0.04356	0.00006	−1.5	2.4	7.2	10
10/2005	#4	0.04373	0.00008	+0.1	1.9	4.2	6
09/2005	#4	0.04346	0.00003	0.0	0.7	3.9	31
08/2005	#1	0.04292	0.00004	+2.6	0.9	6.0	31
08/2005	#4	0.04279	0.00006	−0.4	1.4	4.7	12
07/2005	#2	0.04261	0.00005	−1.1	1.8	4.5	7
06/2005	#2	0.04438	0.00005	−0.6	1.7	5.0	10
05/2005	#3	0.04450	0.00002	+0.1	1.0	2.3	7
03/2005	#3	0.04497	0.00007	−3.1	1.9	7.2	14
02/2005	#4	0.04376	0.00006	−0.1	1.2	2.1	4
$CaSO_4$ $\delta^{34}S_{VCDT}$ +6.5‰							
03/2006	#1	0.04311	0.00008	+4.3	1.5	4.6	11
01/2006	#1	0.04341	0.00007	+9.3	1.5	4.6	10
09/2005	#4	0.04302	0.00005	+7.4	1.1	2.0	3
08/2005	#4	0.04210	0.00006	+5.1	1.6	4.2	8
07/2005	#2	0.04249	0.00005	+6.5	1.9	6.6	12
05/2005	#3	0.04437	0.00003	+6.5	0.5	2.3	19
03/2005	#3	0.04478	0.00007	+6.2	1.9	7.2	14
$CaSO_4{\cdot}2H_2O$ $\delta^{34}S_{VCDT}$ +9.9‰							
03/2006	#1	0.04334	0.00006	+8.4	1.1	3.9	14
01/2006	#1	0.04354	0.00005	+11.7	1.3	4.1	10
09/2005	#3	0.04388	0.00032	+15.5	7.6	10.8	3
08/2005	#3	0.04267	0.00011	+7.3	2.5	5.0	5
07/2005	#2	0.04258	0.00008	+9.9	2.2	3.5	3
05/2005	#3	0.04447	0.00002	+10.0	0.5	2.7	34
03/2005	#3	0.04486	0.00010	+9.2	2.3	5.1	6
$(NH_4)_2SO_4$ $\delta^{34}S_{VCDT}$ + 2.9‰							
03/2006	#1	0.04350	0.00008	+2.9	2.6	7.5	8
01/2006	#1	0.04378	0.00015	+6.2	4.6	16.7	13
09/2005	#4	0.04377	0.00056	+5.5	13.1	13.1	2
08/2005	#4	0.04263	0.00011	+2.8	2.4	5.8	5
Na_2SO_4 $\delta^{34}S_{VCDT}$ + 5.4‰							
03/2006	#1	0.04309	0.00011	+7.0	2.4	6.7	9
01/2006	#1	0.04323	0.00008	+3.9	2.2	8.1	15
K_2SO_4 $\delta^{34}S_{VCDT}$ +9.8							
03/2006	#1	0.04281	0.00008	+10.3	2.4	7.1	10
01/2006	#1	0.04341	0.00015	+9.4	2.1	9.3	12
$MgSO_4{\cdot}xH_2O$ 1–2 wt.% H_2O $\delta^{34}S_{VCDT}$ −0.8‰							
03/2006	#1	0.04281	0.00008	−2.7	1.6	5.5	13
01/2006	#1	0.04312	0.00013	+2.3	1.9	6.6	13
$MgSO_4{\cdot}7H_2O$ $\delta^{34}S_{VCDT}$ +3.1‰							
03/2006	#1	0.04302	0.00010	+1.6	3.1	9.1	10
01/2006	#1	0.04310	0.00011	+4.1	2.4	7.5	11
Cysteine $\delta^{34}S_{VCDT}$ +21.7‰							
03/2006	#1	0.04380	0.00010	+23.3	2.6	7.2	9
01/2006	#1	0.04407	0.00006	+20.6	2.2	7.7	11

The $^{34}S/^{32}S$ ratios are the uncorrected ratios measured with the NanoSIMS. $\delta^{34}S_{VCDT}$ is calculated according to formula 4. σ is the standard deviation. #: number of measurements.

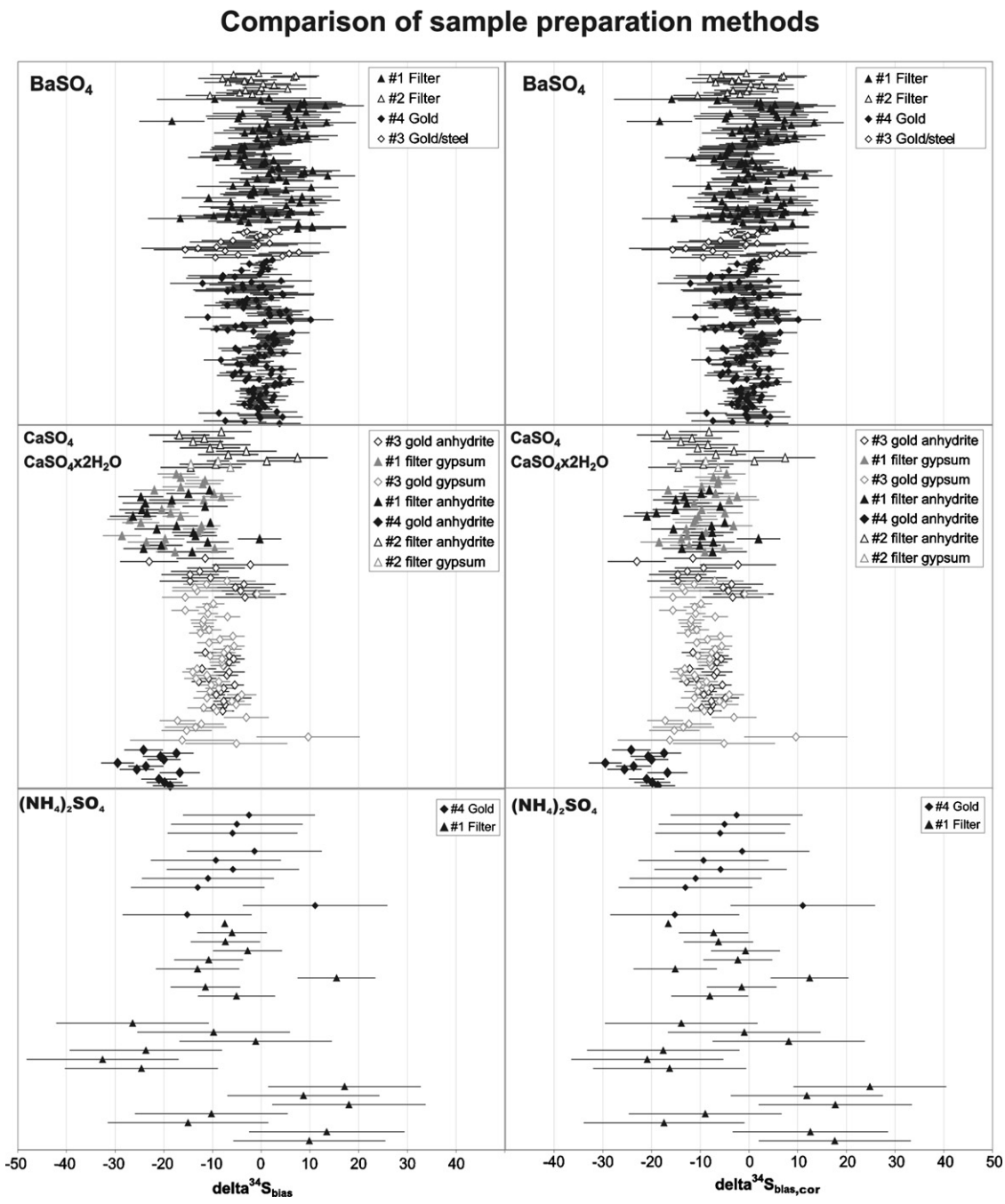

Fig. 6. Comparison of sample preparation methods. Measured IMF $\delta^{34}S_{bias}$ of $BaSO_4$, $CaSO_4$, $CaSO_4{\cdot}2H_2O$ and $(NH_4)_2SO_4$ for different sample preparation methods. The data shown in this figure are from 11 separate sessions with different instrument tunings and show excellent long-term reproducibility for more than 1 year. Errors are 1σ and include the grain-to-grain reproducibility in a given session and the counting statistical error (σ_τ). The left side shows $\delta^{34}S_{bias}$ which is not corrected for the grain size dependence ($a=0$) for sample preparation method #1, the right side shows corrected data ($a=-1.6\,\mu m^{-1}$). It is clearly visible that accounting for the grain size dependence improves the reproducibility (specifically for $CaSO_4$ and $CaSO_4{\cdot}H_2O$). After correcting the grain size dependence, the only significant difference between the sample preparation methods is a higher IMF in favor of ^{32}S for anhydrite for sample preparation method #4 due to increased charging. The charging of the grains is visible in the SEM image in Fig. 3 by the white stripes.

ticles for which no close-up images were taken (i.e., particles that have not been exposed to high electron doses). Only the latter have been taken into account for calculating the IMF of $(NH_4)_2SO_4$ listed in Table 3 and all further data analysis (note that only 3 points of this data series can be plotted in Fig. 8, as all other particles had not been imaged at all prior to SIMS analysis).

With the data given in Table 3 (averages of matrix-specific offsets over all sessions) we have calculated $\delta^{34}S_{VCDT}$ values of all individual measurements (Table 6 and Fig. 7). It can be clearly seen that the inferred $\delta^{34}S_{VCDT}$ values are consistent within error over all sessions for the different sample preparation methods, if method #4 is disregarded. This justifies use of a session-independent matrix-specific IMF correction

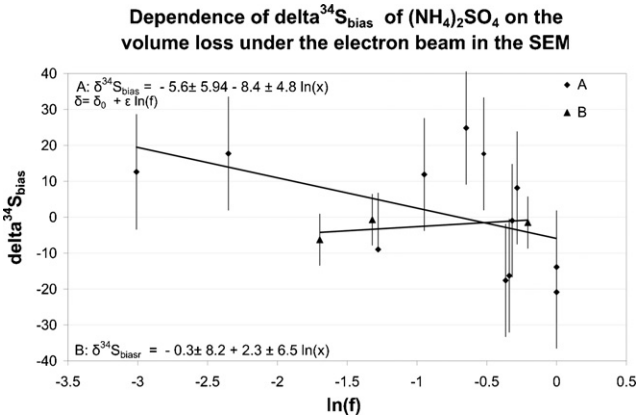

Fig. 7. Correlation between δ^{34}S and volume loss of ammonium sulfate triggered by electron bombardment in the SEM. f: fraction of the remaining substrate. A linear regression of δ^{34}S vs. ln(f) yields a slope of -8.4 ± 4.8‰ for particles that were exposed to high electron doses in the SEM (A) and no significant correlation for particles of which no close-up image was taken (B).

together with the session-dependent correction from $BaSO_4$ measurements. Changing from one sample holder to another does not seem to influence the IMF significantly as long as the distance between sample and extraction lens is kept at the same distance. The problems with the accuracy of the HMR approach that have been observed by Riciputi [22] for polished sections are masked by the large grain-to-grain variations on each filter, that are accounted for when calculating σ_T.

The grain-to-grain reproducibility, σ_R (see Eq. (6) for definition), achieved for the different sample preparation methods is listed in Table 4. For comparison we have also performed S-isotopic measurements on thin sections and ultra microtome sections. Here all the spots analyzed on the same sample agree in most cases within the counting statistical error, which is typically 2‰. This shows, that the poor grain-to-grain reproducibility accomplished on powdered standards is not due to instrumental tuning conditions, which would also affect other types of samples analyzed in the same analytical session. For individual grain measurements the reproducibility does not strongly depend on the sample preparation method; for $BaSO_4$, $CaSO_4$, and $CaSO_4{\cdot}H_2O$ it is between 2‰ and 6‰, for the other samples slightly larger (5–8‰,). But as Table 6 shows, when calculating averages for a given sample type in each session, the accuracy of $\delta^{34}S_{VCDT}$ is clearly better, namely, ∼2‰. For submicrometer-sized grains a better grain-to-grain reproducibility can be expected because of less charging and less pronounced topographic effects. This is evident, e.g., from the distribution of $\delta^{34}S_{VCDT}$ values associated with sea salt sulfates measured by NanoSIMS, which show a pronounced peak around 23‰ with a width of ∼3‰ [2]. This would constrain the grain-to-grain reproducibility of aerosol particles to about 1–2‰.

As sample preparation method #1 is least destructive for aerosol samples and achieves the highest sample throughput, this method was chosen to investigate the matrix dependence of the IMF of $^{34}S/^{32}S$ in more detail.

3.2. Matrix dependence of the IMF

Sulfur in atmospheric aerosol particles can be detected in a variety of minerals as well as internally mixed soot-sulfur particles and organic particles. This requires a large set of standards to correct for the IMF of $^{34}S/^{32}S$. If the whole set of standards would be measured with each individual aerosol sample, the measurement procedure would be very time-consuming. Moreover, it is not always possible to find a standard that matches the actual matrix of the aerosol particle, as complex sulfate mixtures, which are quite frequent among aerosol particles, are not commercially available. Therefore, to measure the $^{34}S/^{32}S$ in the whole range of atmospheric aerosol, a good understanding of the variations in the IMF in different S-bearing minerals is essential.

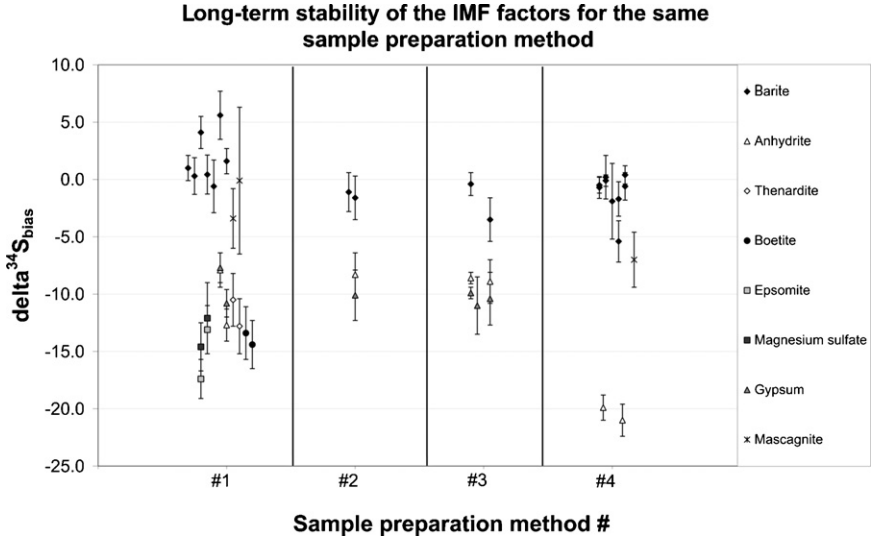

Fig. 8. Matrix-specific IMF of $\delta^{34}S(x)_{bias}$ in different sulfate standards for the different sample preparation methods. Each data point represents the average $\delta^{34}S_{bias}$ value in one of the 11 measurement sessions with different instrument tunings. The data in this plot indicate excellent long-term reproducibility over more than 1 year.

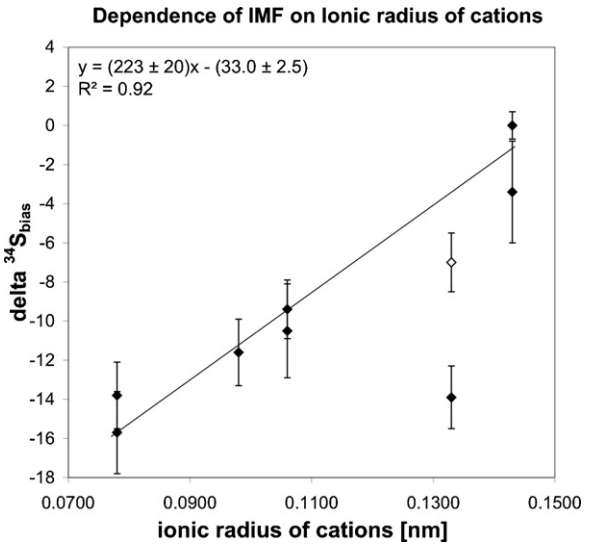

Fig. 9. Dependence of $\delta^{34}S_{bias}$ on the ionic radius of the cations of different sulfates. The solid line is the weighted linear regression of all data points except the one in the lower right (K_2SO_4). With the exception of K_2SO_4 there is a very good correlation between these two quantities. K_2SO_4 presented analytical difficulties, as the filter surface was partially destroyed during sample preparation. One grain of K_2SO_4 is trustworthier than other grains as it was displaced onto the $MgSO_4$ filter during sample preparation and therefore analyzed on a flat intact filter surface. This grain is indicated as an open square and used for the line fit.

The following discussion focuses on the investigation of the IMF of $^{34}S/^{32}S$ in samples prepared by method #1. The average IMF relative to $BaSO_4$ ($\delta^{34}S_{bias}$) is -9.7 ± 1.3‰ for gypsum and anhydrite. The more negative IMF of anhydrite compared to barite is consistent with results presented by Eldridge et al. [12] and McKibben et al. [16] for measurements with the SHRIMP ion microprobe. Na_2SO_4 and K_2SO_4 have a relative IMF of -11.6 ± 1.7‰ and -13.9 ± 1.6‰, respectively. The relative IMF of $\delta^{34}S$ in epsomite and magnesium sulfate is -14.6 ± 1.3‰. The relative IMF of $^{34}S/^{32}S$ in cysteine is -13.5 ± 1.7‰ and that of $(NH_4)_2SO_4$ is -3.4 ± 1.4‰. Because only $(NH_4)_2SO_4$ particles that had not received high electron doses in the SEM were used to calculate the IMF, this value can be considered accurate.

The $\delta^{34}S_{bias}$ correlates very well with the ionic radius R_i of the cations (Fig. 9). A weighted linear regression yields $\delta^{34}S_{bias} = (223 \pm 20)R_i - (33.0 \pm 2.5)$. With the exception of K_2SO_4, the measured $\delta^{34}S_{bias}$ of all sulfates can be predicted with an accuracy of better than 2‰ from a weighted linear regression (Table 3). As we have pointed out before, uncertainties in the relative IMF of $^{34}S/^{32}S$ due to QSA are generally smaller than ±2‰, i.e., QSA cannot account for the observed range in IMF of 15‰. If we correct our data for QSA using the idealized formula by [23] one finds $\delta^{34}S_{bias} = (205 \pm 20)R_i - (30.0 \pm 2.5)$ which differs only marginally from the regression line without consideration of QSA. E.g., the difference in the IMF of $^{34}S/^{32}S$ between sulfates with $R_i = 0.08$ nm and sulfates with $R_i = 0.14$ nm changes only from 13.4‰ to 12.3‰. Therefore, even for sulfates not studied here it seems feasible to predict the IMF correction with an uncertainty that can be considered small compared to the precision of individual grain measurements. We note that K_2SO_4 does not follow the observed correlation, even if the error in the IMF is considered. However, the measurements on K_2SO_4 turned out to be extremely difficult because the conductive gold coating of the filter, and the filter itself was partially destroyed during the handling of this standard with the micro-manipulator. As a consequence, no grains were found on flat, horizontal filter surfaces. This affects the IMF, as secondary ions from tilted surfaces have different trajectories through the instrument. Thus, these data should be viewed with great caution. However, one grain was displaced onto the $MgSO_4$ filter during the sample preparation and, therefore, measured on a flat and horizontal filter surface. This grain is indicated as an open square in Fig. 9. The grain lies close to the expected trend line, even if only the counting statistical error σ_p is considered.

Over a period of several months the relationships established for the IMF of $^{34}S/^{32}S$ in different minerals for the same sample preparation method remained stable (Table 3, Figs. 6 and 7). Therefore, it is sufficient to measure $BaSO_4$ standards in each individual session together with the aerosol samples and to inter-compare all necessary standards at regular time intervals.

4. Summary and conclusions

We have explored the IMF of $^{34}S/^{32}S$ measurements on individual sulfate grains with different chemical composition and on one amino acid with the NanoSIMS ion microprobe. Grain-to-grain reproducibility of grains with identical chemical composition is relatively poor, typically around 5‰ for micron-sized grains and between 2‰ and 5‰ for submicron-sized grains, while accuracy upon averaging measurements of several grains is typically 2‰. Precision is worst for materials that undergo partial decomposition in the SEM or for comparatively large grains with complex topography. The IMF of $^{34}S/^{32}S$ varies by ∼15‰ between the sulfates studied here. The IMF of $^{34}S/^{32}S$ in different sulfates relative to $BaSO_4$ depends only marginally on the sample preparation method (except if large grain assemblies are studied), and turned out to be constant over all measurement sessions. Sufficiently precise S-isotope measurements are thus possible with the measurement of one isotope standard only (e.g., $BaSO_4$). The good correlation between IMF and ionic radius of the cations permits inference of IMF corrections even for sulfates for which no isotope standard is available. The IMF correction requires detailed knowledge (size, mineralogy) about each grain analyzed, and therefore an accurate coordinate transformation from the SEM to the NanoSIMS. For grains that are not pressed into the substrate, the charging of particles, and therefore the IMF of $^{34}S/^{32}S$ increases with the size of the particles. This, however, can be corrected properly as long as the sample matrix, the particle size, and the average grain size of the $BaSO_4$ standard are known.

Despite limitations in precision, the NanoSIMS technique is a novel and useful tool for the isotope analysis of individual atmospheric particles. Due to the small size (0.1−2.5 μm) and limited sulfur content (<17%) of most aerosol grains it is the only tech-

nique capable of doing so. Given the range of S-isotopic ratios in aerosol bulk samples, the achievable grain-to-grain reproducibility and accuracy of a few per mil for the measurement of the $^{34}S/^{32}S$ ratio in individual aerosol particles is sufficient to investigate physical and chemical processes related to aerosol formation and transport. For aerosol particles that can be identified based on chemical composition or morphological features such as sea salt or mineral dust particles, the analysis of several grains with identical composition can give even more precise and accurate results [2].

Acknowledgements

We thank Smail Mostefaoui and Elmar Gröner for their help with the NanoSIMS analyses and Joachim Huth for support on the SEM. We thank Dr. Mathias Gehre, UFZ Leipzig and Dr. Andrea Stögbauer, Geologisch-Paläontologisches Institut und Museum der Westfälischen Wilhelms-Universität Münster, for providing reference values for our in-house standards. We acknowledge the comments by an anonymous reviewer which helped to improve this manuscript. This research is funded by the Max Planck Society.

References

[1] H.R. Krouse, V.A. Grinenko (Eds.), Stable isotopes: natural and anthropogenic sulfur in the environment, SCOPE, vol. 43, Wiley, Chichester, 1991.
[2] B. Winterholler, P. Hoppe, M.O. Andreae, S. Foley, Appl. Surf. Sci. 252 (2006) 7128.
[3] M.J. Whitehouse, B.S. Kamber, C.M. Fedo, A. Lepland, Chem. Geol. 222 (2005) 112.
[4] S.J. Mojzsis, C.D. Coath, J.P. Greenwood, K.D. McKeegan, T.M. Harrison, Geochim. Cosmochim. Acta 67 (2003) 1635.
[5] M. Chaussidon, F. Albarede, S.M.F. Sheppard, Earth Planet. Sci. Lett. 92 (1989) 144.
[6] J.P. Greenwood, L.R. Riciputi, H.Y. McSween, L.A. Taylor, Geochim. Cosmochim. Acta 64 (2000) 1121.
[7] B.A. Paterson, L.R. Riciputi, H.Y. McSween, Geochim. Cosmochim. Acta 61 (1997) 601.
[8] L.R. Riciputi, D.R. Cole, H.G. Machel, Geochim. Cosmochim. Acta 60 (1996) 325.
[9] J. Peevler, M. Fayek, K.C. Misra, L.R. Riciputi, J. Geochem. Explor. 80 (2003) 277.
[10] C.K. Shearer, G.D. Layne, J.J. Papike, M.N. Spilde, Geochim. Cosmochim. Acta 60 (1996) 2921.
[11] J.F. Luhr, M.A.V. Logan, Geochim. Cosmochim. Acta 66 (2002) 3303.
[12] C.S. Eldridge, W. Compston, I.S. Williams, J.L. Walshe, R.A. Both, Int. J. Mass Spectrom. Ion Process. 76 (1987) 65.
[13] M.A. McKibben, C.S. Eldridge, Econ. Geol. 90 (1995) 228.
[14] C.S. Eldridge, N. Williams, J.L. Walshe, Econ. Geol. 88 (1993) 1.
[15] C.S. Eldridge, W. Compston, I.S. Williams, R.A. Both, J.L. Walshe, H. Ohmoto, Econ. Geol. 83 (1988) 443.
[16] M.A. McKibben, C.S. Eldridge, A.G. Reyes, in: C.G. Newhall, R.S. Punongbayan (Eds.), Sulfur isotopic systematics of the June 1991 Mount Pinatubo eruptions: a SHRIMP ion microprobe study, PHIVOLCS and University of Washington Press, Seattle and London, 1996, p. 825.
[17] C. Floss, F.J. Stadermann, J.P. Bradley, Z.R. Dai, S. Bajt, G. Graham, A.S. Lea, Geochim. Cosmochim. Acta 70 (2006) 2371.
[18] L.R. Riciputi, B.A. Paterson, R.L. Ripperdan, Int. J. Mass Spectrom. 178 (1998) 81.
[19] A.A. Gurenko, M. Chaussidon, H.-U. Schmincke, Geochim. Cosmochim. Acta 65 (2001) 4359.
[20] R.L. Hervig, Rapid Commun. Mass Spectrom. 16 (2002) 1774.
[21] G. Slodzian, Appl. Surf. Sci. 231–232 (2004) 3.
[22] L.R. Riciputi, Rapid Commun. Mass Spectrom. 10 (1996) 282.
[23] G. Slodzian, M. Chaintreau, R. Dennebouy, A. Rousse, Eur. Phys. J.-Appl. Phys. 14 (2001) 199.
[24] G. Slodzian, F. Hillion, F.J. Stadermann, E. Zinner, Appl. Surf. Sci. 231–232 (2004) 874.
[25] F. Hillion, B. Daigne, F. Girard, G. Slodzian, in: A. Benninghoven, et al. (Eds.), Secondary Ion Mass Spectrometry SIMS IX, John Wiley & Sons Ltd., Chichester, 1994, p. 254.
[26] P. Hoppe, A. Besmehn, Astrophys. J. 576 (2002) L69.
[27] S. Mostefaoui, P. Hoppe, Astrophys. J. 613 (2004) L149.
[28] H. Busemann, A.F. Young, C.M.O'D. Alexander, P. Hoppe, S. Mukhopadhyay, L.R. Nittler, Science 312 (2006) 727.
[29] T. Ding, S. Valkiers, H. Kipphardt, P. De Bievre, P.D.P. Taylor, R. Gonfiantini, R. Krouse, Geochim. Cosmochim. Acta 65 (2001) 2433.
[30] T.B. Coplen, J. Phys. Chem. Ref. Data 30 (2001) 701.
[31] K.A. Baublys, S.D. Golding, E. Young, B.S. Kamber, Rapid Commun. Mass Spectrom. 18 (2004) 2765.
[32] N.V. Grassineau, D.P. Mattey, D. Lowry, Anal. Chem. 73 (2001) 220.
[33] S. Ono, B. Wing, D. Rumble, J. Farquhar, Chem. Geol. 225 (2006) 30.
[34] C.T. Pillinger, Int. J. Mass Spectrom. Ion Process. 118–119 (1992) 477.
[35] D.E. Crowe, J.W. Valley, K.L. Baker, Geochim. Cosmochim. Acta 54 (1990) 2075.
[36] C.S. Eldridge, J.L. Walshe, W. Compston, I.S. Williams, R.A. Both, H. Ohmoto, Econ. Geol. 84 (1989) 453.
[37] S.P. Kelley, A.E. Fallick, P. McConville, A.J. Boyce, Scan. Microsc. 6 (1992) 129.
[38] J.L. Mann, W.R. Kelly, Rapid Commun. Mass Spectrom. 19 (2005) 3429.